ICNMM2010-30530

ANALYTICAL VELOCITY AND TEMPERATURE DISTRIBUTIONS FOR FLOW IN MICROCHANNELS OF VARIOUS CROSS-SECTIONS

S. Shahsavari
PhD Student
Mechatronic Systems Engineering
Simon Fraser University
sshahsav@sfu.ca

E. Kjeang
Assistant Professor
Mechatronic Systems Engineering
Simon Fraser University
ekjeang@sfu.ca

M. Bahrami
Assistant Professor
Mechatronic Systems Engineering
Simon Fraser University
mbahrami@sfu.ca

ABSTRACT

Analytical solutions are presented for velocity and temperature distributions of laminar fully developed flow of Newtonian, constant property fluids in micro/minichannels for a wide variety of cross-sections. The considered geometries include hyper-elliptical channels and regular polygon ducts, which covers several common shapes. The analysis is carried out under the conditions of constant axial wall heat flux with uniform peripheral heat flux at a given cross section. The boundary conditions are applied using a linear least-squares point matching technique to minimize the residual between the actual and the modeled values on the boundary of the channel. Hydrodynamic and thermal characteristics of the flow are derived; these include pressure drop and local and average Nusselt numbers. The proposed results are successfully verified with existing analytical solutions from literature for a variety of channel cross-sections. The present study provides analytical-based compact solutions for velocity and temperature fields that are essential for basic designs, parametric studies, and optimization analyses required for many thermofluidic applications.

NOMENCLATURE

a	=	Hyperellipse major axis, m
A_C	=	Cross-sectional area, m^2
c_p	=	Specific heat
b	=	Hyperellipse minor axis, m
D_h	=	Hydraulic diameter, $4A/\Gamma_c$, m
f	=	Fanning friction factor
fRe	=	Poiseuille number
k	=	Conductivity
m	=	Number of sides in regular polygonal ducts
Nu	=	Nusselt number
n	=	Exponent in hyperellipse formula
P	=	Pressure, N/m^2
$q^"$	=	Heat Flux, W/m^2
Re	=	Reynolds number
s	=	Half the length of the sides in polygonal ducts, m
T	=	Temperature, K
T^*	=	Dimensionless temperature
u	=	Axial velocity, m/s
u^*	=	Dimensionless velocity
Greek symbols		
α	=	Diffusivity
Γ_c	=	Perimeter, m
ε	=	Cross-sectional aspect ratio, $\varepsilon = b/a$
η	=	Non-dimensional coordinate, $\eta = r/a$
μ	=	Viscosity, $N.s/m^2$
ρ	=	Density, kg/m^3
Subscript		
$\sqrt{A}$	=	Square root of cross-sectional area
w	=	Wall
b	=	Bulk

INTRODUCTION

Advances in micro fabrication technologies make it possible to make microchannels with various cross-sections in microfluidic devices. The convective flow and heat transfer in these channels, apart from their theoretical interest, are of considerable practical importance due to practical applications including the thermal management of electronic devices. The

developments in the microelectromechanical devices naturally require cooling systems that are equally small. Among the novel methods for thermal management of the high heat fluxes found in microelectronic devices, microchannels are the most effective at heat removal [1]. In addition, porous materials can be modeled as networks of microscale conduits; thus, transport properties of porous structures are closely related to the geometry of the considered microchannels. A proper understanding of fluid flow and heat transfer in these microscale systems is therefore essential for their design and operation.

Different methods have been used in the literature to analyze the problem of fully developed laminar flow in non-circular channels, such as analogy method, complex variables method, conformal mapping method, finite difference method, and point matching method. The typical difficulty for obtaining an analytical solution for this problem by means of the well known classical techniques resides in the impossibility of the separation of variables. An additional difficulty is due to the non regular two-dimensional characteristic of the cross section.

Sparrow and Haji-Sheikh [2] proposed a method of least squares matching of boundary values for fully developed laminar flow in ducts of arbitrary cross section. Tyagi [3] analyzed the steady laminar forced convection problem of heat transfer in fully developed flow of liquids through a certain class of channels including equilateral triangular and elliptic tube, using complex variables technique. Shah and London [4] surveyed the literature on analytical solution and alternate methods to study such transport phenomena and interpret the results for twenty five different geometries. Shah [5] presented a least squares matching technique to analyze fully developed laminar fluid flow and heat transfer in ducts of arbitrary cross section. Abdel-Wahed and Attia evaluated hydrodynamic and thermal characteristics of fully developed laminar flow in an arbitrarily shaped triangular duct using a finite difference technique [6]. Maia et al [7] solved heat transfer problem in thermally developing laminar flow of a non-Newtonian fluid in elliptical ducts by using the generalized integral transform technique. They transformed the axes algebraically from the Cartesian coordinate system to the elliptical coordinate system in order to avoid the irregular shape of the elliptical duct wall. However, this method cannot be used in more complex geometries for which transformation is not possible. Furthermore, none of the aforementioned studies presented closed form relations for the velocity and temperature distributions in such complex geometries. In fact, accurate information on the velocity and temperature fields are particularly important in devising efficient strategies in a host of engineering applications such as microfluidic, lab-on-chip devices, and fuel cell technologies, to name a few. An in-depth knowledge of velocity distribution plays a key role in determining other transport properties of microchannels such as heat and mass transfer coefficients. As such, having a generalized solution for the velocity distribution in microchannels is of great value. Tamayol and Bahrami [9] approximated the velocity distribution of fully developed laminar flow in straight channels of regular polygon and hyperellipse cross-section, using the matching point technique. However, they did not solve the temperature problem.

In this study, analytical solutions are presented for velocity and temperature distributions of laminar fully developed flow of Newtonian, constant property fluids in micro/minichannels in both hyperelliptical and polygonal mini/microchannels. The considered geometries include i) hyper-elliptical channels, encompassing concave/convex shapes from star-shaped, rhombic, elliptical , rectangular with round corners, and rectangular, and ii) regular polygon ducts, which covers several common shapes from equilateral triangular, squared, pentagonal, hexagonal, to circular. The proposed solution is presented in a single unique format that covers all the above-mentioned cross-sections.

In order to find the temperature distribution, the energy equation should be solved. Since there is a convective term in the energy equation, we have to find the velocity distribution by solving the momentum equation. In this paper, we first derive the governing equations and find a general solution for ducts with arbitrary cross sections. Then by applying the constant heat flux boundary condition we find the velocity and temperature distribution for polygonal and hyper-elliptical cross sections.

GOVERNING EQUATIONS

Momentum Equation

The liquid flows in minichannels and microchannels in the absence of any wall surface effects, such as the electrokinetic or electroosmotic forces, is not expected to experience any fundamental changes from the continuum theory employed in macrofluidic applications [11]. Gad-el-Hak [12] argued that liquids such as water should be treated as continuous media with the results obtained from classical theory being applicable in channels larger than 1 μm. Thus, existing solutions for large scale ducts are also applicable to microchannels. In this paper, fully developed, laminar flow of constant properties and incompressible fluids is considered in microchannels with constant hyperelliptical and polygonal cross-section. Under these conditions, the momentum equation in cylindrical coordinates reduces to Poisson's equation [13]:

$$\frac{\partial^2 u}{\partial r^2} + \frac{1}{r}\frac{\partial u}{\partial r} + \frac{1}{r^2}\frac{\partial^2 u}{\partial \theta^2} = \frac{1}{\mu}\frac{dP}{dz} \qquad (1)$$

where μ is the fluid viscosity. Due to geometrical symmetry, only a portion of the cross-section is considered in the analysis, as shown in Figs. 1 and 2.

Applicable boundary conditions for hyper-elliptical channels are:

$$\left.\frac{\partial u}{\partial \theta}\right|_{\theta=\frac{\pi}{2}} = 0 , \quad \left.\frac{\partial u}{\partial \theta}\right|_{\theta=0} = 0 , \qquad u(r_0) = 0 \qquad (2)$$

The first two boundary conditions are obtained from the existing symmetry in the hyper-ellipse geometry, and the last one is the no slip condition on the wall.

The boundary of a hyperellipse in the first quadrant is described by Eq. (3).

$$r_o = \frac{a}{((\cos\theta)^n + (\sin\theta/\varepsilon)^n)^{1/n}} , \quad 0 < \varepsilon = \frac{b}{a} \leq 1 \qquad (3)$$
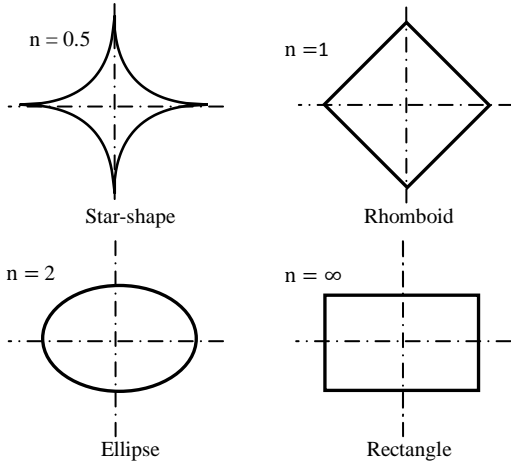
FIGURE 1. HYPERELLIPTICAL CROSS SECTIONS.

FIGURE 3. SOLUTION DOMAIN FOR REGULAR POLYGON AND ELLIPSE.

where ε is the aspect ratio, a and b are the major and minor axes of the cross-section, respectively.

Similarly, the boundary conditions for regular polygon cross-section are:

$$\left.\frac{\partial u}{\partial \theta}\right|_{\theta=\frac{\pi}{m}} = 0 \, , \quad \left.\frac{\partial u}{\partial \theta}\right|_{\theta=0} = 0, \quad u(r_0) = 0 \tag{4}$$

where the boundary for the specified domain in Figure 3 can be described by:

$$r_o = \frac{s}{\tan(\frac{\pi}{m}) \cos\theta} \tag{5}$$

where m is the number of sides of a regular polygon, and s is one half of each side.
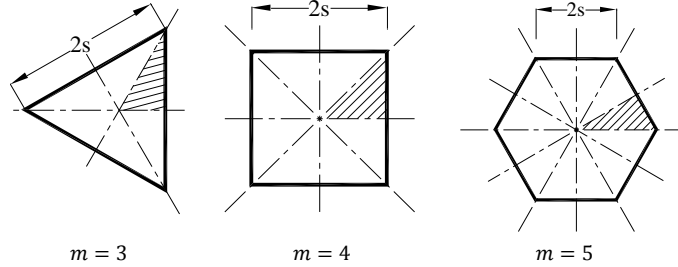

FIGURE 2. REGULAR POLYGON.

The general solution of the Poisson's equation, Eq. (3), in the cylindrical coordinate is [14]:

$$u = A_1 + B \ln r + \frac{r^2}{4\mu}\left(\frac{dP}{dz}\right) \tag{6}$$
$$+ \sum_{k=1}^{\infty}(C_k r^k + D_k r^{-k})(E_k \cos k\theta + F_k \sin k\theta)$$

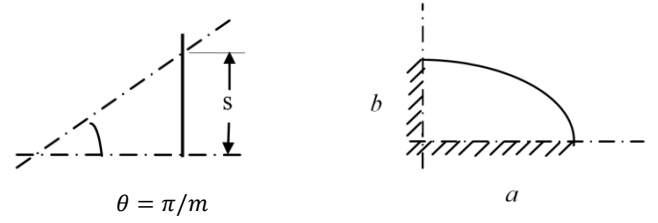The unknown coefficients, A_1, B, C_k, D_k, E_k, and F_k, should be calculated by applying the boundary conditions, Eq. (2) and Eq. (4). For the solution to be applicable in a general form, the governing equations should be non-dimensionalized. The dimensionless velocity is defined as:

$$u^* = \frac{u}{-\frac{1}{\mu}\left(\frac{dP}{dz}\right) L_c^2} \tag{7}$$

For a hyperellipse, L_c is the major axis a and for a polygon $L_c = \frac{s}{\sin\frac{\pi}{m}}$. For simplicity, This characteristic length is chosen so that the dimensionless radial component, $\eta = \frac{r}{L_c}$, satisfy $0 \leq \eta \leq 1$. After applying the symmetry boundary conditions, the non-dimensionalized velocity reduces to:

$$u^* = A_1 - \frac{1}{4}\eta^2 + \sum_{i=1}^{\infty} C_i \eta^{mi} \cos mi\theta \tag{8}$$

where for hyperelliptic cross-section $m = 2$ and for polygonal cross-section m is the number of sides of the polygon. The difference between the two geometries arises from the location of the symmetry line.

Applying no-slip boundary condition, the remaining unknown coefficients can be determined. Here a point matching technique is use to apply the boundary conditions. To approximate the solution to the velocity problem, Eq. (8), the infinite series can be truncated at a finite number of terms k. The k points are selected on the periphery Γ, the boundary condition is satisfied exactly at these k points to determine the k unknown coefficients of the truncated series. The velocity and temperature distributions are then obtained in a closed-form series. The limitation of this method is that by increasing the number of points on the boundary, one cannot obtain a more accurate result since the degree of the polynomial is increased, which may result in overfitting.

To overcome this problem, the least squares method is used. The least squares method differs from the point-matching method in that more than k points along the boundary are employed to determine k unknown coefficients in the truncated series. Therefore, we will have an over-determined linear system of equations. The coefficients are evaluated by minimizing the mean squared error of the boundary conditions at j points $(j > k)$.

Energy Equation

In addition to idealizations made for the momentum equation, for simplifying the energy equation, axial heat conduction,

viscous dissipation, and thermal energy sources within the fluid are neglected. The applicable differential energy equation for laminar hydrodynamically and thermally developed flow is

$$\frac{\partial^2 T}{\partial r^2} + \frac{1}{r}\frac{\partial T}{\partial r} + \frac{1}{r^2}\frac{\partial^2 T}{\partial \theta^2} = \frac{u}{\alpha}\frac{\partial T}{\partial z} \tag{9}$$

The associated thermal boundary condition is considered as axially constant heat transfer rate per unit channel length, with peripherally constant heat flux. For this boundary condition and fully developed flow, it can be shown that

$$\frac{\partial T}{\partial z} = \frac{\partial T_m}{\partial z} = \frac{q''\Gamma_c}{\rho A_c u_m c_p} \tag{10}$$

where u_m, the mean velocity is defined as

$$u_m = \frac{\int_{A_c} u dA_c}{A_c} \tag{11}$$

Substituting Eq. (8) into (9) yields

$$\frac{\partial^2 T}{\partial r^2} + \frac{1}{r}\frac{\partial T}{\partial r} + \frac{1}{r^2}\frac{\partial^2 T}{\partial \theta^2}$$
$$= \frac{q''PL_c^2}{\alpha \rho A_c u_m^* c_p}\left[A_1 - \frac{1}{4}\eta^2 + \sum_{i=1}^{\infty} C_i \eta^{mi} \cos mi\theta\right] \tag{12}$$

or in the dimensionless form:

$$\frac{\partial^2 T^*}{\partial \eta^2} + \frac{1}{\eta}\frac{\partial T^*}{\partial \eta} + \frac{1}{\eta^2}\frac{\partial^2 T^*}{\partial \theta^2} = A_1 - \frac{1}{4}\eta^2$$
$$+ \sum_{i=1}^{\infty} C_i \eta^{mi} \cos mi\theta \tag{13}$$

where T^* is defined as

$$T^* = \frac{T}{\frac{q''\Gamma_c L_c^2}{kA_c u_m^*}} \tag{14}$$

The solution of Eq. (13) is expressed as the sum of separate particular and homogeneous solutions as follows

$$T^* = T_p^* + T_h^* \tag{15}$$

For a particular solution, it is easily verified by direct substitution that the following expression is a satisfactory particular solution [14]:

$$T_p^* = A_1 \frac{\eta^2}{4} - \frac{\eta^4}{64} + \sum_i C_i \frac{\eta^{mi+2}}{4(mi+1)} Cosmi\theta \tag{16}$$

and the general homogeneous solution is

$$T_h^* = d_0 + \sum_j \eta^j (d_j Cosj\theta + e_j Sinj\theta) \tag{17}$$

The symmetry boundary conditions for the thermal problem in the domain shown in Figure 3 are determined by Eq. (18).

$$\left.\frac{\partial T_h^*}{\partial \theta}\right|_{\theta=\frac{\pi}{m}} = 0 , \quad \left.\frac{\partial T_h^*}{\partial \theta}\right|_{\theta=0} = 0 \tag{18}$$

Appling the symmetry boundary conditions, we obtain: $e_j = 0$ and $j = m, 2m, 3m, ...$ and we can rewrite Eq. (17) as follows:

$$T_h^* = d_0 + \sum_{j=1}^{\infty} d_j \eta^{mj} Cosmj\theta \tag{19}$$

Therefore, the temperature distribution can be found from Eq. (20).

$$T^* = d_0 + \sum_{j=1}^{\infty} d_j \eta^{mj} Cosmj\theta + A_1 \frac{\eta^2}{4} - \frac{\eta^4}{64} \tag{20}$$
$$+ \sum_{i=1}^{\infty} C_i \frac{\eta^{mi+2}}{4(mi+1)} Cosmi\theta$$

Applying the last boundary condition, constant heat flux per unit area, we should have the following constraint on the channel's wall

$$\left.\frac{\partial T^*}{\partial n}\right|_{\eta=\eta_o} = \frac{A_c^* u_m^*}{\Gamma_c^*} \tag{21}$$

where Γ_c^*, A_c^* are dimensionless perimeter and cross-sectional area defined by $\Gamma_c^* = \Gamma_c/L_c$ and $A_c^* = A_c/L_c^2$. The dimensionless form for defining the outer boundary is $\eta_o = \frac{r_o}{L_c}$ and the normal gradient of temperature is:

$$\frac{\partial \bar{T}}{\partial n} = \hat{n}.\vec{\nabla}T \tag{22}$$

where $\hat{n}$ is the normal vector of the boundary defined by $F(\eta, \theta) = 0$:

$$F(\eta,\theta) = \begin{cases} \eta\left[(cos\theta)^n + (\frac{sin\theta}{\varepsilon})^n\right]^{\frac{1}{n}} - 1 & \text{hyper-ellipse} \\ \eta \cos(\theta) - \cos\frac{\pi}{m} & \text{regular polygon} \end{cases} \tag{23}$$

Using a similar approach employed to solve the momentum equation, the infinite series in Eq. (20) is truncated. The coefficients d_i are calculated by the least-squares point matching technique. By this technique, we could achieve a reasonable accuracy, with maximum error of 6%, using just one or two terms of the series.

RESULTS

The coefficient in Eqs. (8) and (20) are reported in tables 1 and 2. Using just two terms of the infinite series in the solutions to the velocity and temperature distributions resulted in maximum error of 6% in applying the boundary value for the various geometries that were studied in this work. Table 3 shows the closed form velocity and temperature relations for some examples from the studied geometries.
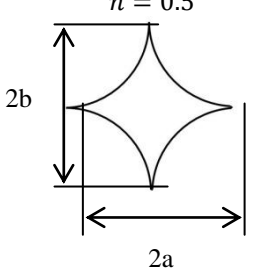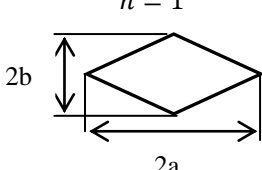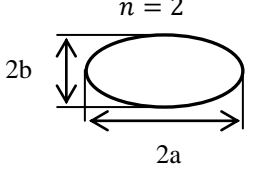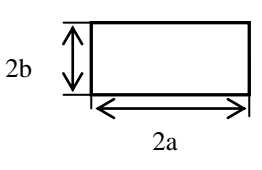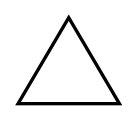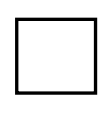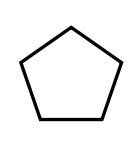
TABLE 1. COEFFICIENTS IN EQS. (8) AND (20) FOR HYPERELLIPTICAL CHANNELS

$n = 40$, rectangle							
	$\varepsilon = 0.2$	$\varepsilon = 0.25$	$\varepsilon = 0.4$	$\varepsilon = 0.5$	$\varepsilon = 0.6$	$\varepsilon = 0.8$	$\varepsilon = 1$
A_1	0.0198	0.0309	0.0768	0.1141	0.1533	0.2293	0.2948
C_1	0.2600	0.2617	0.2401	0.2062	0.1649	0.0781	0.0000
C_2	-0.0250	-0.0369	-0.0617	-0.0665	-0.0657	-0.0577	-0.0479
d_1	-0.0068	-0.0083	-0.0084	-0.0078	-0.0069	-0.0040	0.000
d_2	-0.0013	-0.0003	0.0000	0.0000	0.0000	0.0000	0.0028

$n = 4$, rectangle with round corner							
	$\varepsilon = 0.2$	$\varepsilon = 0.25$	$\varepsilon = 0.4$	$\varepsilon = 0.5$	$\varepsilon = 0.6$	$\varepsilon = 0.8$	$\varepsilon = 1$
A_1	0.0199	0.0309	0.0755	0.1116	0.1495	0.2231	0.2867
C_1	0.2508	0.2475	0.2192	0.1874	0.1499	0.0712	0.000
C_2	-0.0188	-0.0259	-0.0413	-0.0454	-0.0459	-0.0415	-0.0347
d_1	-0.0076	-0.0088	-0.0088	-0.0085	-0.0077	-0.0046	0.000
d_2	-0.0009	0.0000	0.0000	0.0000	0.0000	0.0000	0.0028

$n = 2$, ellipse							
	$\varepsilon = 0.2$	$\varepsilon = 0.25$	$\varepsilon = 0.4$	$\varepsilon = 0.5$	$\varepsilon = 0.6$	$\varepsilon = 0.8$	$\varepsilon = 1$
A_1	0.0192	0.0294	0.0690	0.1000	0.1324	0.1951	0.250
C_1	0.2308	0.2206	0.1810	0.1500	0.1176	0.0549	0
d_1	-0.0080	-0.0065	-0.0083	-0.0082	-0.0075	-0.0046	0

$n = 1$, rhomboid							
	$\varepsilon = 0.2$	$\varepsilon = 0.25$	$\varepsilon = 0.4$	$\varepsilon = 0.5$	$\varepsilon = 0.6$	$\varepsilon = 0.8$	$\varepsilon = 1$
A_1	0.0151	0.0222	0.0470	0.0647	0.0824	0.1164	0.1474
C_1	0.1980	0.1769	0.1161	0.0833	0.0578	0.0230	0.0000
C_2	0.0421	0.0580	0.0979	0.1133	0.1196	0.1137	0.0963
d_1	-0.0025	-0.0029	0.0000	0.0000	0.0000	0.0000	0.0000

$\varepsilon = 1$, star-shape							
	$n = 0.9$	$n = 0.8$	$n = 0.7$	$n = 0.6$	$n = 0.5$	$n = 0.4$	$n = 0.3$
A_1	0.1282	0.1073	0.0853	0.0631	0.0424	0.0245	0.0115
C_1	0.0000	0.0000	0.0000	0.0000	0.0000	0.0000	0.0000
C_2	0.1191	0.1476	0.1831	0.2267	0.2708	0.2778	0.2520
d_1	0.0000	0.0000	0.0000	0.0000	0.0000	0.0000	0.0000

TABLE 2. COEFFICIENTS IN EQ. (13) FOR POLYGONAL CHANNELS.

$m =$	3	4	5	6	7	8	9	10	20
A_1	0.0833	0.1473	0.1823	0.2024	0.2149	0.2231	0.2288	0.2328	0.2458
C_1	-0.1667	-0.0909	-0.0558	-0.0374	-0.0267	-0.0199	-0.0154	-0.012	-0.0028
C_2	0.0000	0.0103	0.0095	0.0075	0.0058	0.0046	0.0036	0.0030	0.0007
d_1	0.0000	0.0000	0.0000	0.0000	0.0006	0.0004	0.0003	0.0002	0.0000

TABLE 3. EXAMPLES OF DEVELOPED VELOCITY AND TEMPERATURE DISTRIBUTIONS

cross-section	aspect ratio	velocity profile (u^*)	temperature profile ($\bar{T} = T^* - T_b^*$)
$n = 0.5$ 2b 2a	$\varepsilon = 1$	$0.0424 - \dfrac{1}{4}\eta^2$ $+ 0.2708\,\eta^4\cos 4\theta$	$-0.0009 + 0.0424\dfrac{\eta^2}{4} - \dfrac{\eta^4}{64}$ $+ 0.2708\,\dfrac{\eta^6}{20}Cos4\theta$
$n = 1$ 2b 2a	$\varepsilon = 0.5$	$0.0647 - \dfrac{1}{4}\eta^2$ $+ 0.0833\,\eta^2\cos 2\theta$ $+ 0.1133\,\eta^4\cos 4\theta$	$-0.0014 + 0.0647\dfrac{\eta^2}{4} - \dfrac{\eta^4}{64}$ $+ 0.0833\dfrac{\eta^4}{12}Cos2\theta$ $+ 0.1133\dfrac{\eta^6}{20}Cos4\theta$
$n = 2$ 2b 2a	$\varepsilon = 0.5$	$0.1 - \dfrac{1}{4}\eta^2 + 0.15\,\eta^2\cos 2\theta$	$-0.0037 + 0.1\dfrac{\eta^2}{4} - \dfrac{\eta^4}{64}$ $-0.0082\eta^2 Cos2\theta + 0.15\dfrac{\eta^4}{20}Cos2\theta$
$n = \infty$ 2b 2a	$\varepsilon = 0.5$	$0.1141 - \dfrac{1}{4}\eta^2$ $+ 0.2062\,\eta^2\cos 2\theta$ $- 0.0665\,\eta^4\cos 4\theta$	$-0.0057 + 0.1141\dfrac{\eta^2}{4} - \dfrac{\eta^4}{64}$ $- 0.0078\eta^2 Cos2\theta$ $+ 0.2062\dfrac{\eta^4}{12}Cos2\theta$ $- 0.0665\dfrac{\eta^6}{20}Cos4\theta$
(triangle)	-	$0.0833 - \dfrac{1}{4}\eta^2$ $- 0.1667\,\eta^3\cos 3\theta$	$-0.0024 + 0.0833\dfrac{\eta^2}{4} - \dfrac{\eta^4}{64}$ $- 0.1667\dfrac{\eta^5}{16}Cos3\theta$
(square)	-	$0.1473 - \dfrac{1}{4}\eta^2$ $- 0.0909\,\eta^4\cos 4\theta$ $+ 0.0103\,\eta^8\cos 8\theta$	$-0.0067 + 0.1473\dfrac{\eta^2}{4} - \dfrac{\eta^4}{64}$ $- 0.0909\dfrac{\eta^6}{20}Cos4\theta$ $+ 0.0103\dfrac{\eta^{10}}{36}\cos 8\theta$
(pentagon)	-	$0.1823 - \dfrac{1}{4}\eta^2$ $- 0.0558\,\eta^5\cos 5\theta$ $+ 0.0095\,\eta^{10}\cos 10\theta$	$-0.0099 + A_1\dfrac{\eta^2}{4} - \dfrac{\eta^4}{64}$ $- 0.0558\dfrac{\eta^7}{24}Cos5\theta$ $+ 0.0095\dfrac{\eta^{12}}{44}Cos10\theta$

Two important characteristics of convective flow in channels are the Poiseuille number and the Nusselt number. The Poiseuille number, f Re, is the common dimensionless number used for analyzing pressure drop in channels and is defined by:

$$fRe = -\frac{1}{\mu}\frac{dP}{dx} \times \frac{A_c^{3/2}}{\Gamma_c u_m} \tag{24}$$

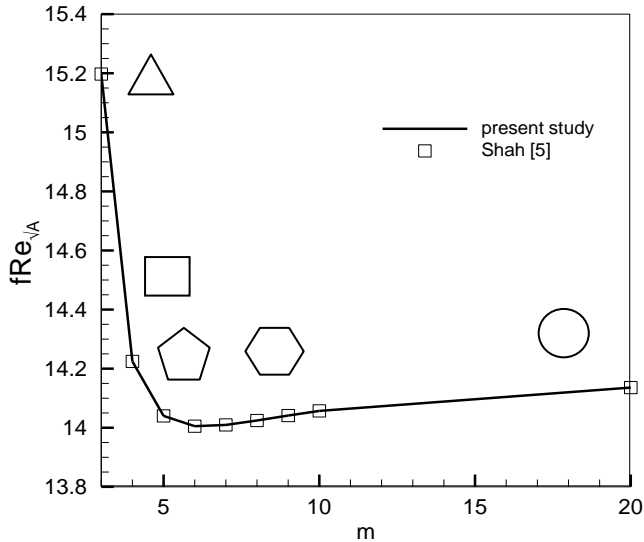Here we have chosen the square root of area as a characteristic length scale, since it can catch up the trend of variation in fRe more consistently than the hydraulic diameter [9,10].

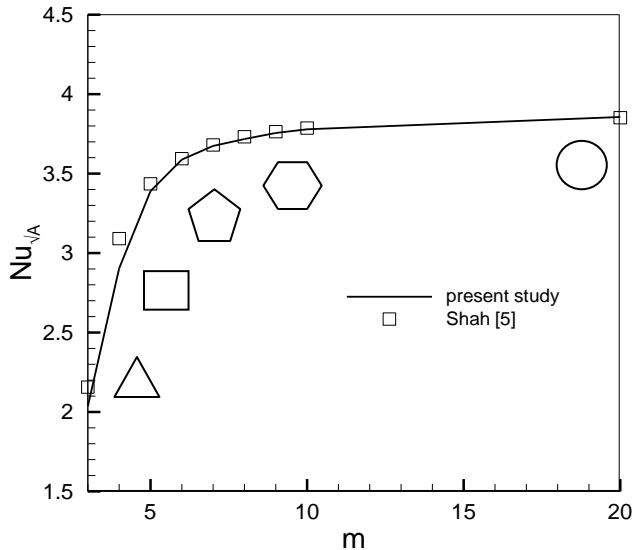FIGURE 4. POISEUILLE NUMBER IN POLYGONAL CHANNELS

FIGURE 5. NUSSELT NEMBER IN POLYGONAL CHANNELS

The Nusselt number, Nu is the ratio of convective to conductive heat transfer normal to the boundary. The local Nusselt number is defined by

$$Nu = \frac{\sqrt{A}}{(T_w - T_b)}\frac{\partial T}{\partial n}\Big|_{r=r_o} \tag{25}$$

where T_w is the wall temperature and T_b is the fluid bulk temperature defined by Eq. (26). The average Nusselt number is defined by using the average wall temperature in Eq. (25).

$$T_b = \frac{\int_{A_c} uT dA_c}{\int_{A_c} u dA_c} \tag{26}$$

The results for the Poiseuille number and Nusselt number are plotted in Figures 4 and 5 for hyperelliptical channel and Figs. 6 and 7 for polygonal channels and are compared with other analytical/numerical data [4,5].
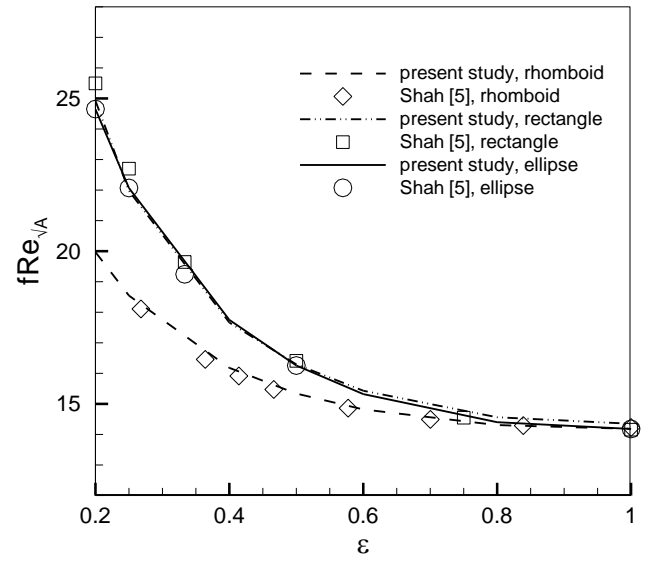

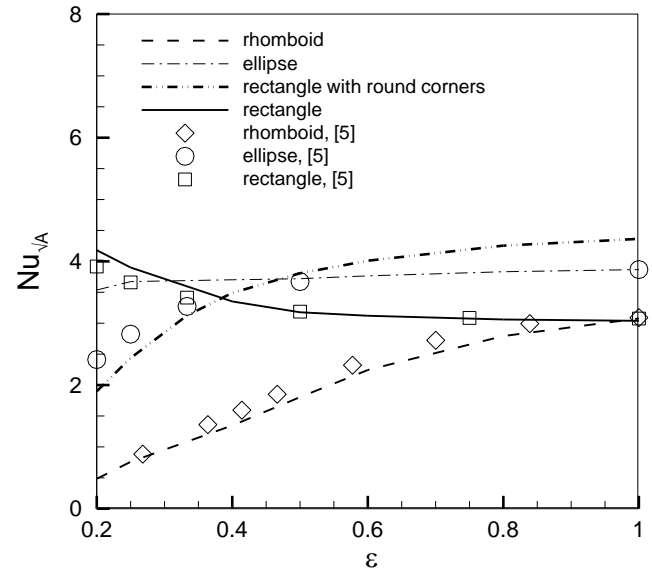FIGURE 6. POISEUILLE NUMBER IN CHANNELS OF HYPERELLIPTIC CROSS-SECTION.

FIGURE 7. NUSSELT NEMBER IN CHANNELS OF HYPERELLIPTIC CROSS-SECTION.

In Figure 8, the local Nusselt number, calculated from Eq. (25), is plotted for channels with star-shape and square cross-section.
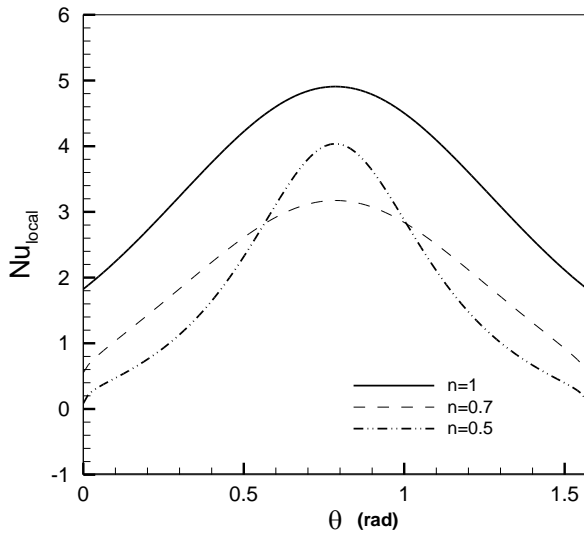

FIGURE 8. LOCAL NUSSELT NEMBER IN HYPERELLIPTIC CHANNELS, $\varepsilon = 1$.

SUMMARY AND CONCLUSIONS

In the present work, analytical solutions are presented for laminar fully developed flow and heat transfer in micro/minichannels of arbitrary cross-sections. The point matching technique is used to apply the boundary condition and the least squares method is employed in order to minimize the error of the boundary values. Velocity and temperature distributions are obtained for various geometries, with different aspect ratios, from which hydrodynamic and thermal characteristics of the flow were calculated. Also, using this method, the local Nusselt numbers are determined. For star-shaped channels, the local Nu near the corners is close to zero, which is due to the fact that in these regions the velocity of the fluid is almost zero as a result of the high wall shear stress.

The geometries that were considered in this study, encompass a wide range of shapes, therefore, the present approach can be considered as a general solution. This model develops compact relations for the velocity and temperature distributions, estimates the pressure drop and the Nusselt number with a good accuracy and therefore provides tools for basic design, parametric studies, and optimization analyses required for microchannel heat exchangers and heat sinks.

REFERENCES

[1] Choondal B. Sobhan and Suresh V. Garimella, 2001, "A Comprehensive Analysis of Studies on Heat Transfer and Fluid Flow in Microchannels", *Microscale Thermophysical Engineering,* **5**, pp. 293–311.

[2] Sparrow, E. M., 1961, "Heat Transfer to Longitudinal Laminar Flow between Cylinders", *Journal of Heat Transfer,* **83,** pp. 415-426

[3] Tyagi, V. P., 1966, "Laminar Forced Convection of a Dissipative Fluid in a Channel", *Journal of Heat Transfer*, pp. 161-169,

[4] Shah, R. K., 1975, "Laminar Flow Friction and Forced Convection Heat Transfer in Ducts of Arbitrary Geometry", *Int. J. Heat and Mass Transfer*, **18**, pp. 849-862

[5] Shah, R. K., London, A. L., 1978, *Laminar Flow Forced Convection in Ducts*, Academic Press, New York

[6] Abdel-Wahed, R. M., Attia, A. E., 1984, "Fully developed laminar flow and heat transfer in an arbitrarily shaped duct", *Wärme-und Stoffübertragung,* **18**, 83-88

[7] Maia, C. R. M., Aparecido, J. B., Milanez, L. F., 2006, "Heat transfer in laminar flow of non-Newtonian fluids in ducts of elliptical section", *International Journal of Thermal Sciences*, **45**, pp. 1066-1072

[8] Erdoğan, M. E., Imrak, C. E., 2005, "The Effects of Duct Shape on the Nusselt Number", *Mathematical and Computational Applications*, **10**, pp. 79-88

[9] Tamayol, A., Bahrami, M., 2009, "Fully-Developed Flow in Microchannels with Hyper-Elliptical Cross-Section", ASME Fluids Engineering Division Summer Meeting

[10] Sadeghi, E., Bahrami, M., Djilali, N., 2008, "Estimation of Nusselt Number in Microchannels of Arbitrary Cross-Section with Constant Axial Heat Flux", ICNMM2008

[11] Kandlikar, S.G., Garimella, S., Li. D., Colin, S., King, M.R., 2006. *Heat Transfer and Fluid Flow in Minichannels and Microchannels*, 1st ed., Elsevier Science & Technology, CA 92101-4495, USA, Chap. 3, pp. 87-100

[12] Gad-el-Hak, M., 1999, "The fluid mechanics of microdevices", *J. Fluid. Eng.*, **121**, 7–33.

[13] White, F.M, 1984, *Viscous Fluid Flow*, McGraw-Hill, New York.

[14] Farlow, S.J., 1993, *Partial Differential Equations for Scientists and Engineers*, Dover Publication INC., NY.

[15] Peng, X.F., 1996, "Convective heat transfer and flow friction for water flow in microchannel structures", *International Journal of Heat and Mass Transfer,* **39**, pp. 2599-2608.